Supplementary Material – Appendix B

for

Infrared spectroscopy of natural *Type Ib* diamond: insights into the formation of *Y*-centers and the early aggregation of nitrogen

Maxwell C. Day[1*], Mike Jollands[2], Francesca Innocenzi[1], Davide Novella[1], Fabrizio Nestola[1], and Martha G. Pamato[1]

[1] Dipartimento di Geoscienze, Università di Padova, 35131 Padova, Italy

[2] Gemological Institute of America (GIA), 50W, 47th Street, New York, NY, 10036, U.S.A.

Data from FTIR spectra recorded *Type Ib* + *IaA* diamonds

Figures B.1 – B.16

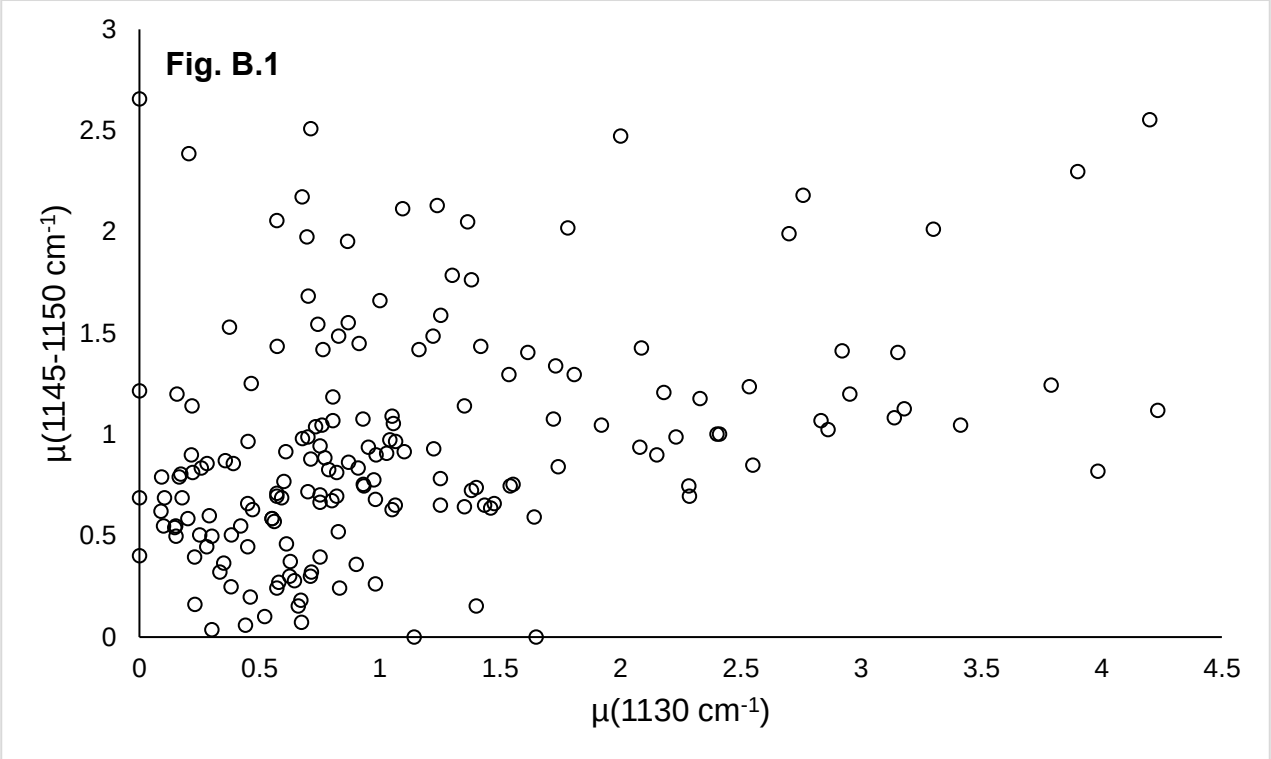

Figure. B.1. A comparison of the thickness normalized absorption μ(1145-1150 cm^{-1}) and μ(1130 cm^{-1}) for the main peaks in the ***Y***- and ***C***-center absorption systems, respectively. The lack of any correlation indicates N_Y and $N_C(Y)$ vary independently and that absorption due to ***Y***-centers is not an artefact of the ***C***-center absorption system related to particular N_{tot} or ***C***-center contents.

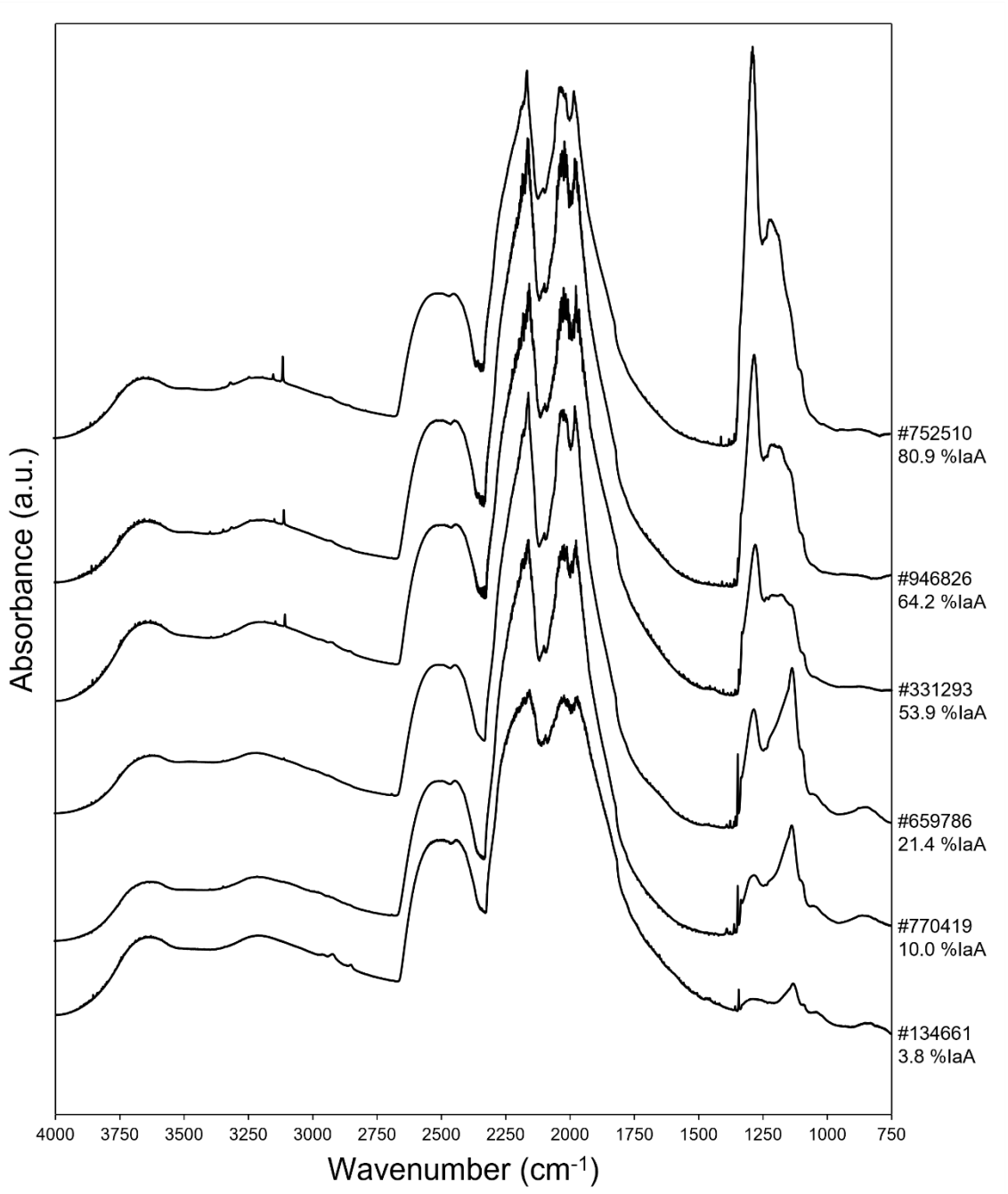

Figure. B.2. FTIR spectra of *Type Ib + IaA* diamonds (data from Table C.2) in the frequency range 4000-750 cm^{-1} plotted as a function of increasing %IaA(Y). Note several peaks from 3400-3100 cm^{-1} due to hydrogen-related defects that were not considered as they are beyond the scope of this work.

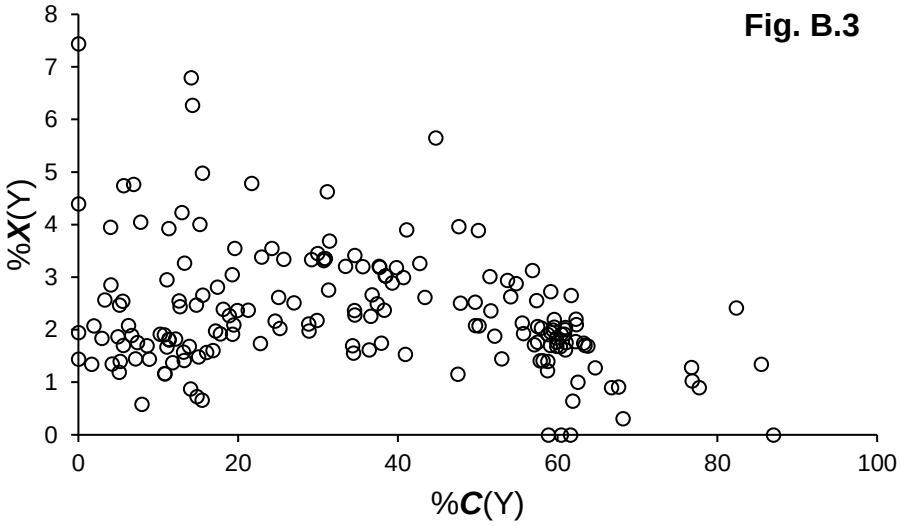

Figure. B.3. Comparison of %***X***(Y) plotted as a function of %***C***(Y). Refer to *Terminology and Nomenclature* for explanations of all terms.

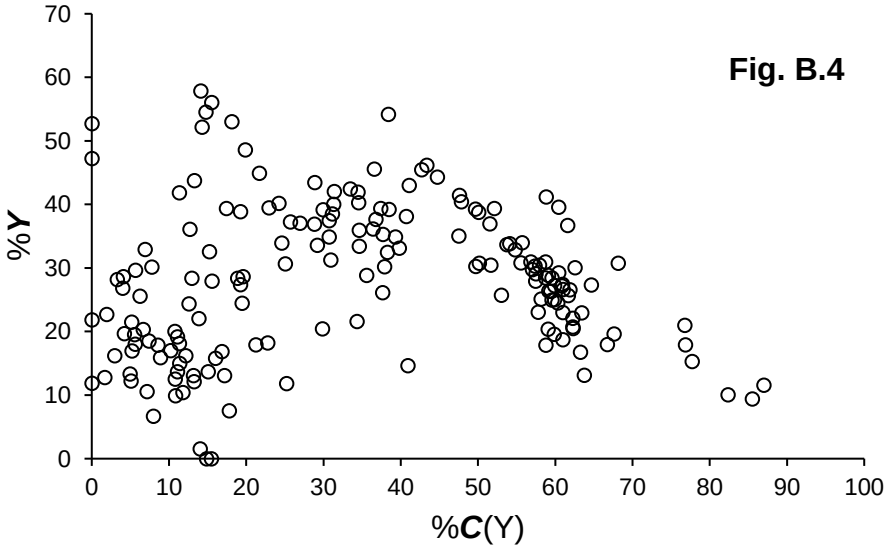

Figure. B.4. Comparison of %***Y*** plotted as a function of %***C***(Y). Refer to *Terminology and Nomenclature* for explanations of all terms.

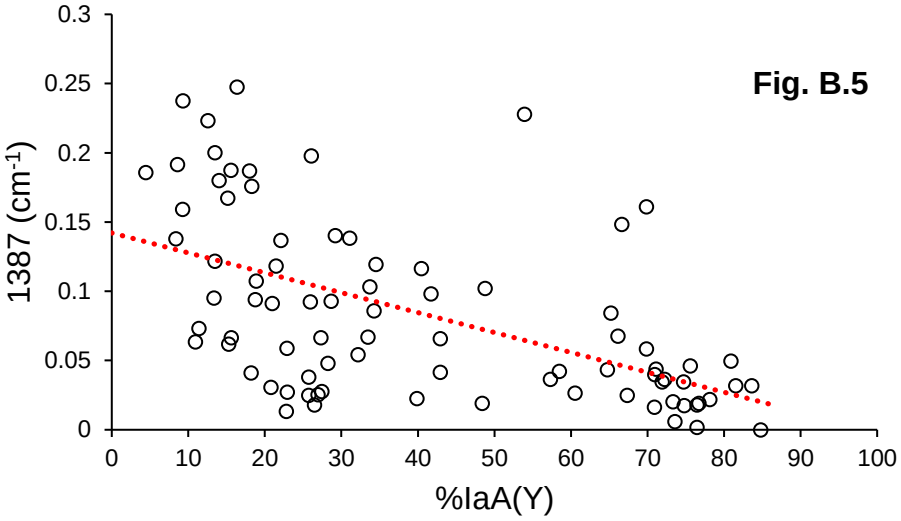

Figure. B.5. Comparison of the normalized 1387 cm^{-1} peak intensity plotted as a function of %IaA(Y). Red dashed line indicates trend determined to be significant at 95% confidence. Refer to *Terminology and Nomenclature* for explanations of all terms.

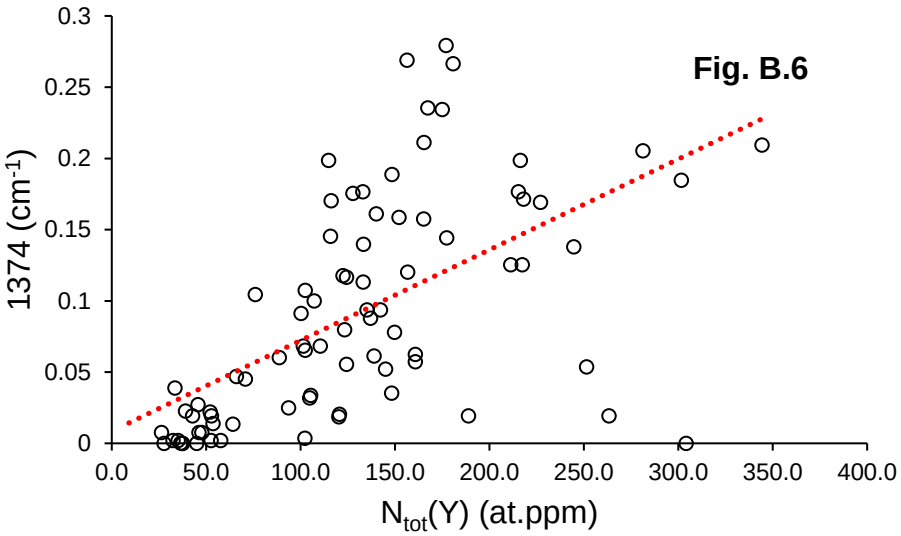

Figure. B.6. Comparison of the normalized 1374 cm^{-1} peak intensity plotted as a function of N_{tot}(Y) (at.ppm). Red dashed line indicates trend determined to be significant at 95% confidence. Refer to *Terminology and Nomenclature* for explanations of all terms.

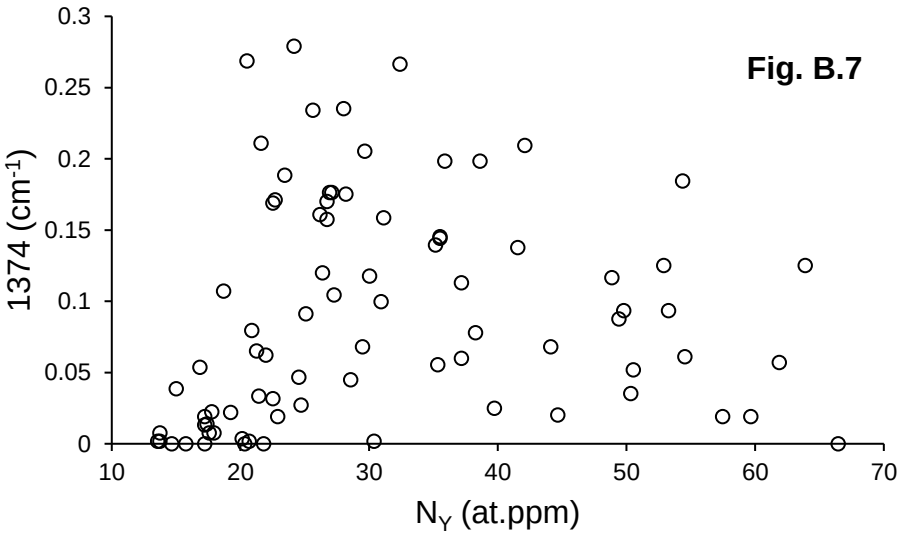

Figure. B.7. Comparison of the normalized 1374 cm^{-1} peak intensity plotted as a function of N_Y (at.ppm). Refer to *Terminology and Nomenclature* for explanations of all terms.

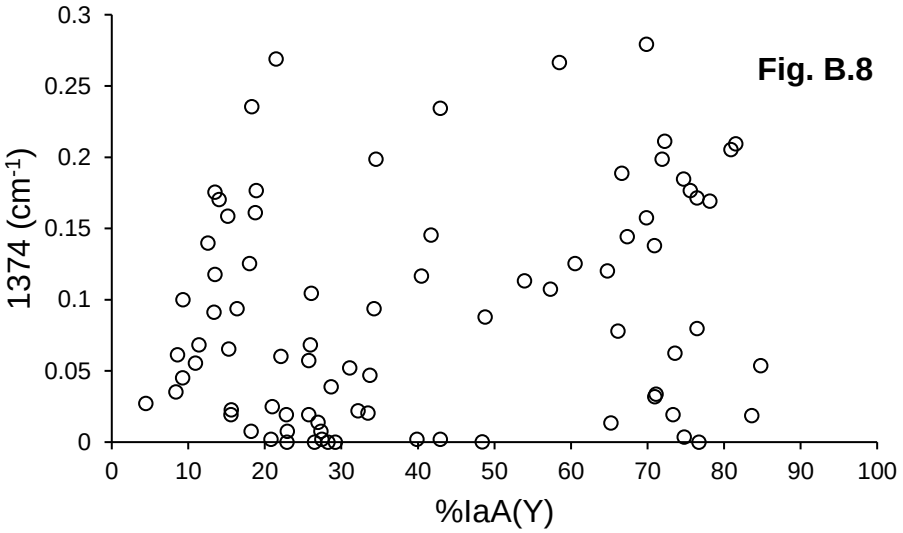

Figure. B.8. Comparison of the normalized 1374 cm^{-1} peak intensity plotted as a function of %IaA(Y). Refer to *Terminology and Nomenclature* for explanations of all terms.

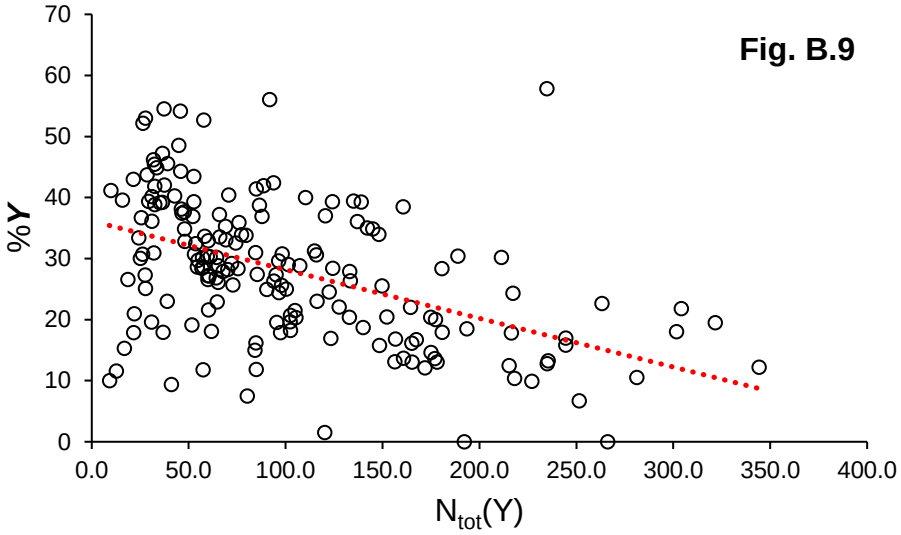

Figure. B.9. Comparison of %***Y*** plotted as a function of N_{tot}(Y) (at.ppm). Red dashed line indicates trend determined to be significant at 95% confidence. Refer to *Terminology and Nomenclature* for explanations of all terms.

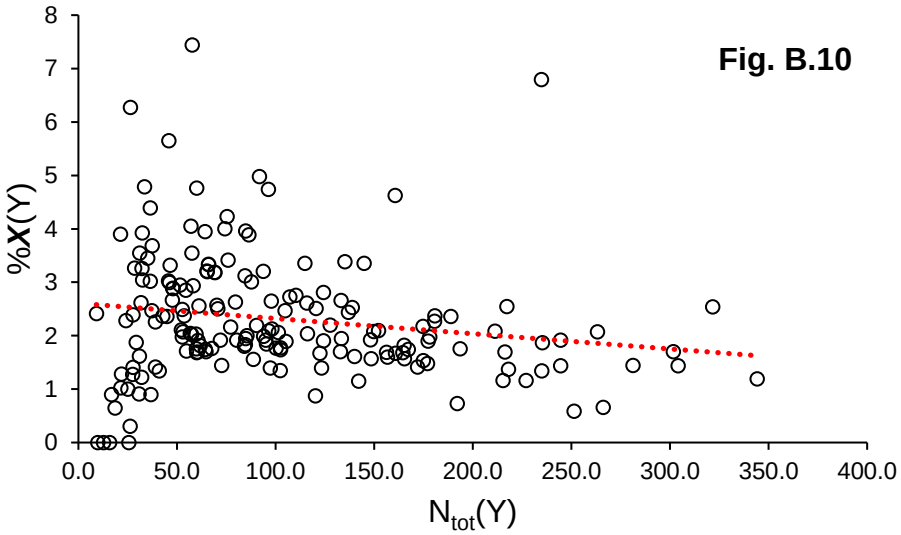

Figure. B.10. Comparison of %***X***(Y) plotted as a function of N_{tot}(Y) (at.ppm). Red dashed line indicates trend determined to be significant at 95% confidence. Refer to *Terminology and Nomenclature* for explanations of all terms.

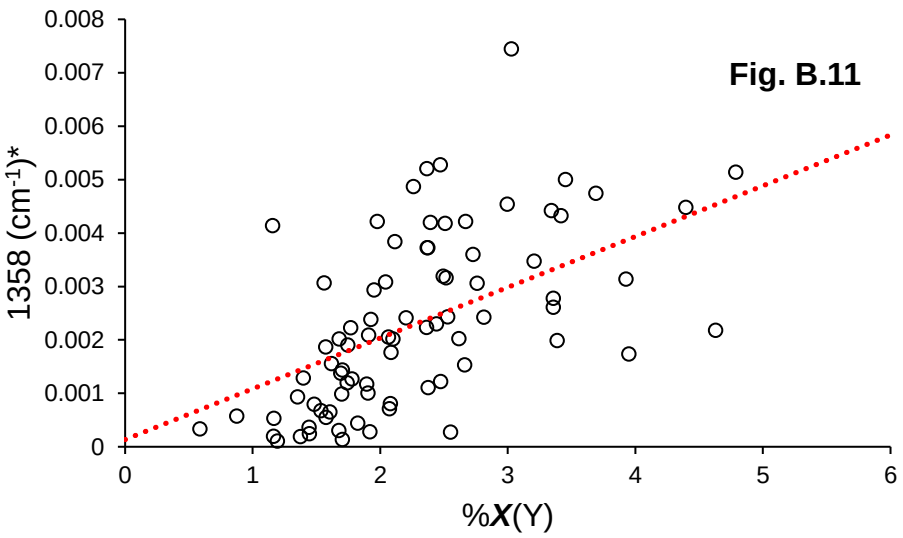

Figure. B.11. Comparison of the 1358 cm^{-1} peak intensity (normalized to $N_{tot}(Y)$) plotted as a function of %***X***(Y). Red dashed line indicates trend determined to be significant at 95% confidence. Refer to *Terminology and Nomenclature* for explanations of all terms.

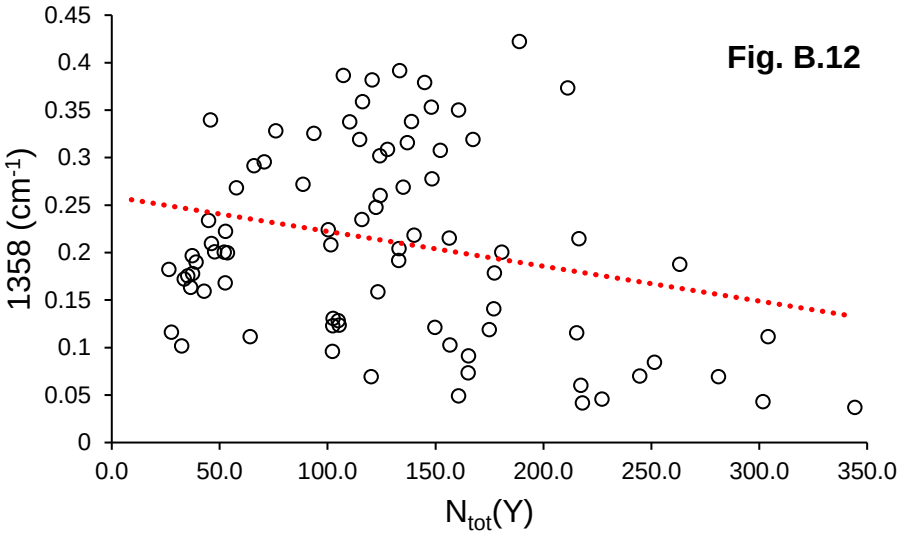

Figure. B.12. Comparison of the normalized 1358 cm^{-1} peak intensity plotted as a function of $N_{tot}(Y)$ (at.ppm). Red dashed line indicates trend determined to be significant at 95% confidence. Refer to *Terminology and Nomenclature* for explanations of all terms.

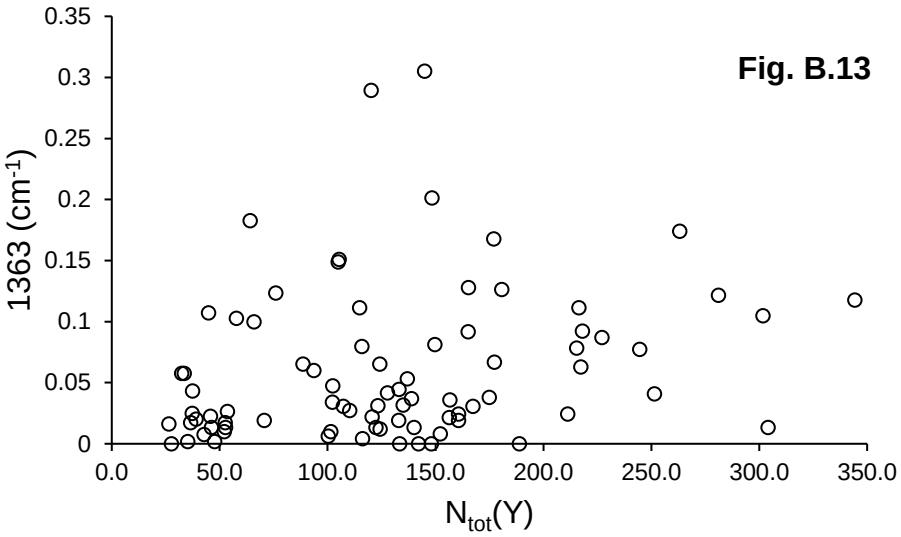

Figure. B.13. Comparison of the normalized 1363 cm^{-1} peak intensity plotted as a function of $N_{tot}(Y)$ (at.ppm). Red dashed line indicates trend determined to be significant at 95% confidence. Refer to *Terminology and Nomenclature* for explanations of all terms.

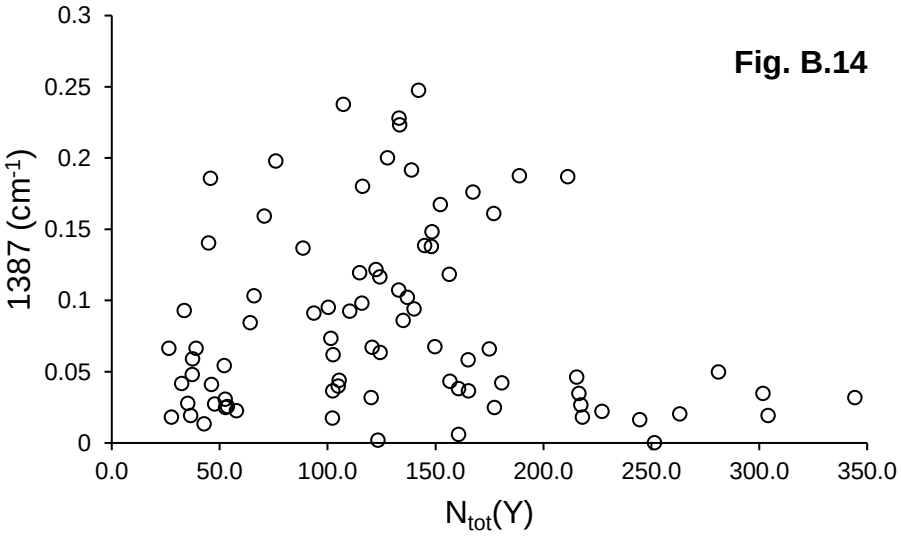

Figure. B.14. Comparison of the normalized 1387 cm^{-1} peak intensity plotted as a function of $N_{tot}(Y)$ (at.ppm). Red dashed line indicates trend determined to be significant at 95% confidence. Refer to *Terminology and Nomenclature* for explanations of all terms.

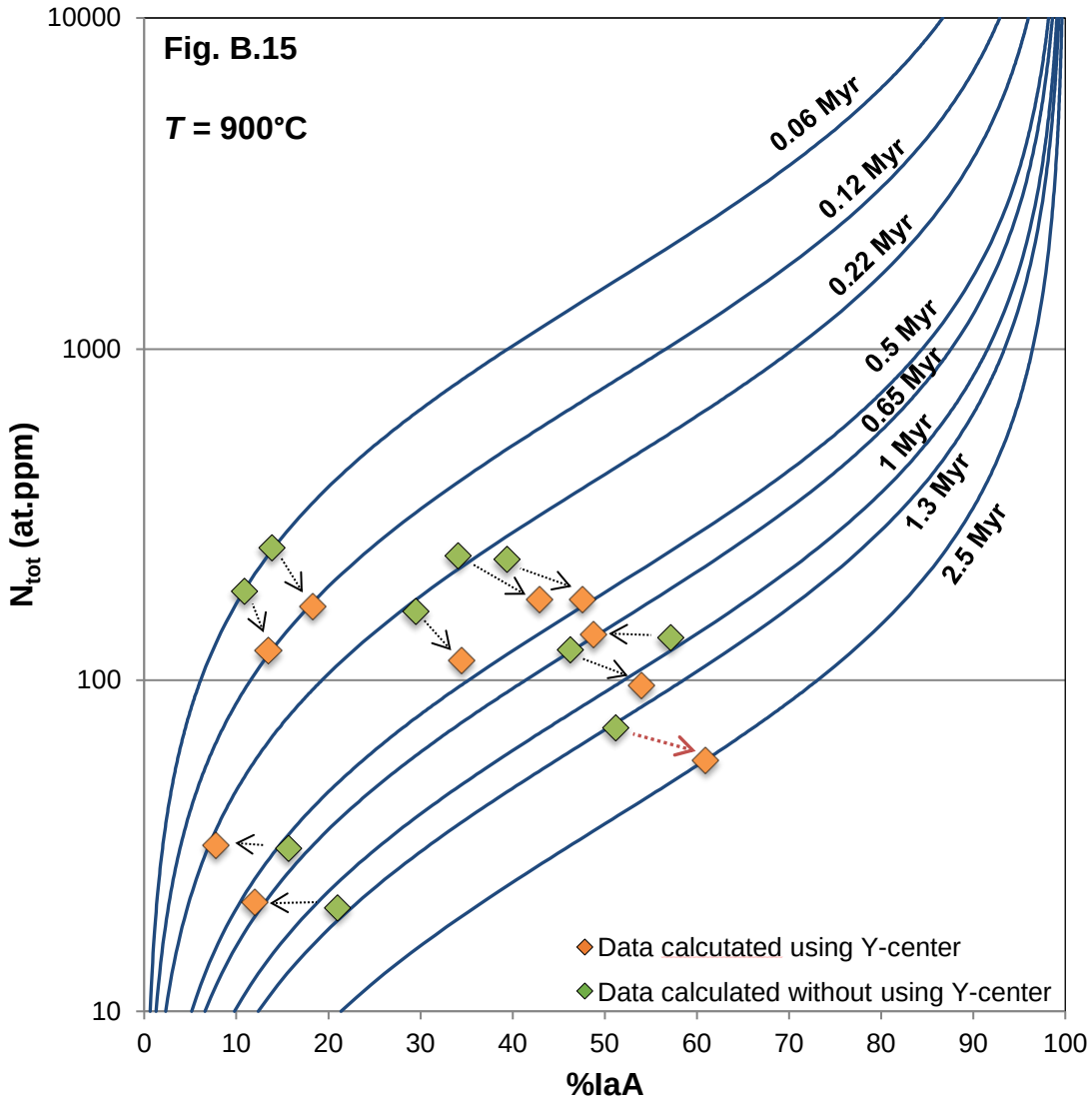

Figure. B.15. Total N content (N_{tot} (at.ppm)) plotted as a function of N-aggregation state (%IaA) where 900°C isotherms (blue lines) are plotted for residence times of 0.06 to 2.5 Myr. To show the effect of ***Y***-centers on calculated mantle residence times or temperatures, N_{tot} and %IaA (green squares), determined without incorporation of ***Y***-centers, and N_{tot}(Y) and %IaA(Y) (orange squares), determined by incorporating ***Y***-centers, are plotted for selected samples. Arrows show the effect of correcting N_{tot} and %IaA (to N_{tot}(Y) and %IaA(Y)) on residence time and temperature. The red arrow represents sample #547284. Where %IaA is overestimated, there is minimal difference between N_{tot} and N_{tot}(Y) (see arrows pointing from right to left). Isotherms were calculated and plotted by modifying the second-order rate equation formula from *DiaMap* (Howell et al. 2012a/b). The activation energy, E_a = 5.5 eV from Kiflawi et al. (1997) was used.

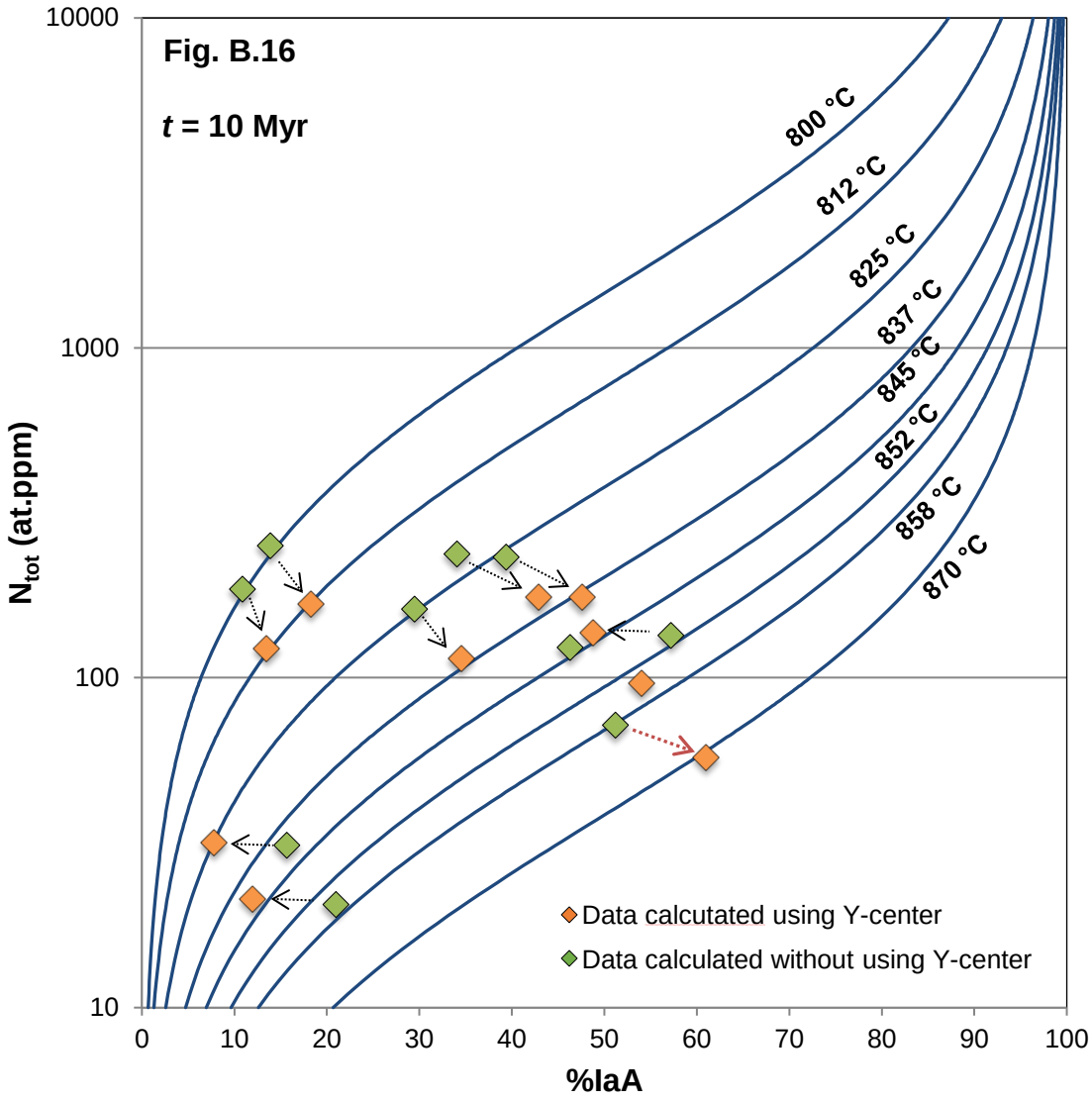

Figure. B.16. Total N content (N_{tot} (at.ppm)) plotted as a function of N-aggregation state (%IaA) where 10 Myr isotherms (blue lines) are plotted for residence temperatures of 800 to 870 °C. To show the effect of ***Y***-centers on calculated mantle residence times or temperatures, N_{tot} and %IaA (green squares), determined without incorporation of ***Y***-centers, and N_{tot}(Y) and %IaA(Y) (orange squares), determined by incorporating ***Y***-centers, are plotted for selected samples. Arrows show the effect of correcting N_{tot} and %IaA (to N_{tot}(Y) and %IaA(Y)) on residence time and temperature. The red arrow represents sample #547284. Where %IaA is overestimated, there is minimal difference between N_{tot} and N_{tot}(Y) (see arrows pointing from right to left). Isotherms were calculated and plotted by modifying the second-order rate equation formula from *DiaMap* (Howell et al. 2012a/b). The activation energy, E_a = 5.5 eV from Kiflawi et al. (1997) was used.